

# Consideration for Polarization of Antennas in Dynamic Body Area Networks at 400 MHz narrow band.

Takahiro Aoyagi

Graduate School of Decision Science and Technology,

Tokyo Institute of Technology

2-12-1-W9-110, Ookayama, Meguro-ku,

Tokyo, Japan

aoyagi@cradle.titech.ac.jp

## ABSTRACT

This paper presents a consideration for directions of both transmitting and receiving antennas in dynamic on-body networks at 403.5 MHz by using FDTD simulation results. The temporal level difference for the six human movements and the six receiving locations are calculated with the antenna directions  $\mathbf{u}$ ,  $\mathbf{v}$ , and  $\mathbf{w}$ . The statistical analysis shows that the overall level variations are well modeled by the log-normal fittings by individual combinations of the transmitting and the receiving antenna directions. It is shown that the UW combination of the antenna direction gives largest received level with smallest deviation, however, the differences between the other combinations are not significant. The results in this paper will be used further investigation for propagation channel modeling of on-body networks.

## Categories and Subject Descriptors

I.6.m [Simulation and Modeling]: Miscellaneous; C.2.m [Computer-Communication Networks]: Miscellaneous; J.3 [Computer Applications]: Life and Medical Sciences

## General Terms

Body Area Networks

## 1. INTRODUCTION

Recently, Body Area Networks (BANs) make great attention for people who want to utilize ICT (information communication technology) into medical or health care purposes. BAN is also one of very fascinating research theme for researchers who are in charge with electromagnetic wave propagations or antennas. For BANs, antennas are very closely attached on or in human body, so it is not easy to design an antenna for BANs which properly works in actual usages. Propagations of BANs are also includes complicated problems to be solved. One of biggest problem is to model dynamic characteristics of propagation channels for BANs. Human motions cause large scale level fluctuations in wearable BAN prop-

agations due to shadowing by human body, and changes of antenna orientations. There have been many studies which are related to dynamic BAN channel propagations and its modelings by measurements or simulations[5][10][6][3][4][7]. In the ref. [5], on-body BAN channel has been characterized by using FDTD (finite difference time domain method[8]) simulations with moving numerical human models generated by an animation software. and channel fluctuations during human walking are calculated at 2.45 GHz. In the ref. [4], a female walking model and a male rising from a chair are added to the simulations, and it has been shown that the simulations and the measurements of slow fading features showed good agreement. In the ref. [3], on-body BAN channels at 403.5 MHz were calculated by FDTD for six human movements. Moreover, in the ref. [3], antenna directions are considered. The diamond shaped markers which indicate antenna directions are attached the numerical human model. However, the polarizations of the antennas were limited to two directions which are parallel to the surfaces of human body, because there wasn't a realistic antenna for BANs which polarization is perpendicular to the surface of human body. Recently, a realistic antenna, which its polarization is perpendicular to the surface of human body, is reported[1]. Although the designed antenna in the ref.[1] is for 2.45 GHz and 950 MHz bands, we can expect such type of antenna for lower frequencies. For the future BAN propagations, we also expect antenna directions and polarizations are optimized for actual use. In this paper, an additional direction, perpendicular to the surface of human body, is added to the previous calculations in [3], and propagation characteristics are discussed from the viewpoint of antenna directions.

## 2. PROPAGATION SIMULATIONS DURING VARIOUS HUMAN MOVEMENTS.

Fig. 1 shows the numerical human model and the diamond shaped antenna location and direction markers. The numerical model and the calculation method are same as in the ref. [3]. The electromagnetic wave propagations have calculated by the FDTD simulations for the 5 mm grid human voxel model at 403.5 MHz. Calculation area is, for example,  $144 \times 438 \times 232$  voxels for walking case, which can be calculated by a workstation with several gigabytes of main memory. The simulations were performed by using an in-house FDTD code. The ten layers perfect matching layer was employed as boundary conditions. Time resolution for dynamic movement of human was 30 frame/s. The an-

Permission to make digital or hard copies of all or part of this work for personal or classroom use is granted without fee provided that copies are not made or distributed for profit or commercial advantage and that copies bear this notice and the full citation on the first page. To copy otherwise, to republish, to post on servers or to redistribute to lists, requires prior specific permission and/or a fee.

PFT 2013, September 30-October 02

Copyright © 2013 ICST 978-1-936968-89-3

DOI 10.4108/icst.bodynets.2013.253510

tennas were represented by the 5 mm-length line elements. Three antenna directions,  $\mathbf{u}$ ,  $\mathbf{v}$ , and  $\mathbf{w}$  are considered in this report, whereas the direction  $\mathbf{w}$  was not considered in the ref. [3]. As shown in the Fig. 1,  $\mathbf{u}$  and  $\mathbf{v}$  represent antennas which have parallel polarization to human skin, and  $\mathbf{w}$  represents antennas which have perpendicular polarization to human skin. In this report, notations such as 'UV' means the direction of the transmitter is oriented for  $\mathbf{u}$ , and the direction of the transmitter is oriented for  $\mathbf{v}$ . Six human movements, walking, sit/standing, running, sleeping, changing-cloth, and weak-walking are considered. The antenna on the abdomen (navel) is set as the transmitter. Other six locations, chest, head, right arm, right ankle, right thigh, and right hand, are set as the receivers.

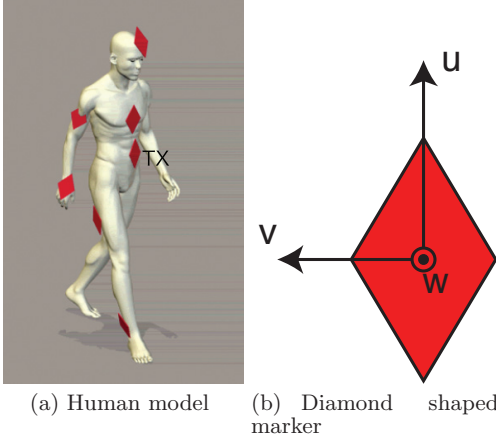


**Figure 1:** Numerical human model used in this study and diamond shaped markers to indicate antenna locations and directions.

### 3. SIMULATION RESULTS: TEMPORAL VARIATION OF RECEIVED LEVEL FOR EACH ANTENNA LOCATIONS.

Fig. 2, Fig. 3, and Fig. 4 show the temporal variations of received level for each receiving antennas during human movements of walking, running, and weak-walking, respectively. In weak-walking movements, which represents a walking motion of aged people, the upper half of the body slightly leans forward and the actions are smaller. Although six movements have been calculated by FDTD, only three of them are presented here for the matter of space. In the figures, the horizontal axis shows number of frames, and the vertical axis shows relative received levels for each receiving antennas (on chest, head, right arm, right ankle, right thigh, and right hand). As mentioned above, notations such as 'UU' show the polarization of the transmitting and receiving antenna. The results of polarization combinations UU, UV, VU, and VV are already presented in the ref. [3]. The results of polarization combination UW, VW, WU, WV, and WW are added in this report. As shown in the figures, the variations of received levels differ among the movements and receiving locations. As described in [3], polarization diversity is useful to improve received levels for these situations. Adding one more polarization  $\mathbf{w}$  may improve the absolute received level for specific situations.

Table 1 shows the mean, maximum, minimum and dynamics (maximum – minimum) of the temporal received levels for all movements by the receiving locations and the combinations of the TX-RX antenna directions. As shown in the table, mean of the received levels mainly changes due to the location of the receiving antennas, as distances between the transmitter and the receivers largely differ among the receiving locations. However, it is shown that the combinations of the TX-RX polarization affects individual locations. For example, for the VV case, the averaged received level for the chest is  $-75.6$  dB, which is maximum in all polarizations. However, for the VV case, the averaged received level for the ankle is  $-114.5$  dB, which is the minimum in all polarizations. As concluded in the ref. [3], polarization diversity is one of most effective technique for this complicated relation among the receiving locations with human movements.

	Chest	Head	Arm	Ankle	Thigh	Hand
Mean	-80.1	-100.9	-93.7	-106.9	-104.4	-98.9
Max	-67.7	-86.6	-79.1	-98.7	-88.0	-78.8
Min	-114.6	-164.1	-117.1	-149.7	-193.8	-158.6
Max-Min	46.9	77.5	37.9	50.9	105.8	79.8
UV	Chest	Head	Arm	Ankle	Thigh	Hand
Mean	-85.9	-111.1	-102.4	-111.9	-95.8	-97.2
Max	-74.5	-93.7	-83.3	-97.7	-84.4	-73.1
Min	-125.3	-188.7	-152.8	-155.6	-139.5	-158.6
Max-Min	50.8	95.0	69.5	57.9	55.1	85.5
UW	Chest	Head	Arm	Ankle	Thigh	Hand
Mean	-81.7	-91.1	-96.2	-103.5	-88.2	-102.2
Max	-68.5	-83.8	-82.4	-92.6	-81.9	-80.6
Min	-128.7	-139.5	-144.0	-142.9	-95.0	-150.7
Max-Min	60.1	55.8	61.6	50.3	13.1	70.1
VU	Chest	Head	Arm	Ankle	Thigh	Hand
Mean	-86.1	-107.5	-97.2	-108.1	-101.8	-94.7
Max	-64.1	-92.6	-85.2	-99.0	-83.8	-83.0
Min	-132.5	-153.0	-138.4	-137.2	-160.4	-128.2
Max-Min	68.4	60.4	53.1	38.3	76.6	45.2
VV	Chest	Head	Arm	Ankle	Thigh	Hand
Mean	-75.6	-102.2	-101.4	-114.5	-94.7	-99.4
Max	-65.8	-89.6	-87.3	-95.9	-84.6	-79.7
Min	-85.8	-169.6	-149.5	-149.4	-139.0	-159.9
Max-Min	20.1	80.0	62.2	53.5	54.3	80.2
VW	Chest	Head	Arm	Ankle	Thigh	Hand
Mean	-90.6	-100.6	-99.9	-99.8	-95.1	-100.5
Max	-66.3	-86.4	-84.6	-91.5	-84.7	-79.2
Min	-155.6	-142.6	-133.1	-110.6	-154.3	-138.6
Max-Min	89.4	56.1	48.5	19.1	69.6	59.4
WU	Chest	Head	Arm	Ankle	Thigh	Hand
Mean	-82.9	-105.1	-96.9	-111.0	-99.4	-96.2
Max	-67.4	-90.2	-86.5	-97.7	-82.0	-81.1
Min	-133.1	-164.5	-143.5	-148.6	-193.1	-141.3
Max-Min	65.6	74.3	57.0	50.9	111.1	60.2
WV	Chest	Head	Arm	Ankle	Thigh	Hand
Mean	-88.5	-114.0	-101.7	-113.3	-96.3	-98.2
Max	-56.9	-96.8	-85.7	-95.7	-84.3	-77.5
Min	-141.3	-155.6	-139.4	-156.0	-150.0	-148.4
Max-Min	84.3	58.8	53.7	60.3	65.7	70.9
WW	Chest	Head	Arm	Ankle	Thigh	Hand
Mean	-81.2	-98.4	-100.0	-105.9	-100.9	-98.9
Max	-58.7	-82.9	-85.7	-97.5	-86.0	-82.5
Min	-146.1	-142.6	-166.1	-180.5	-152.7	-152.5
Max-Min	87.5	59.6	80.4	83.0	66.7	70.0

**Table 1:** Received levels for all movements by sensor locations and polarization combinations.

Table 2 shows the mean, maximum, and dynamics of the received levels for the all movements and the all locations by the combinations of TX-RX antenna directions. As shown in the table, the UW shows highest mean value among all

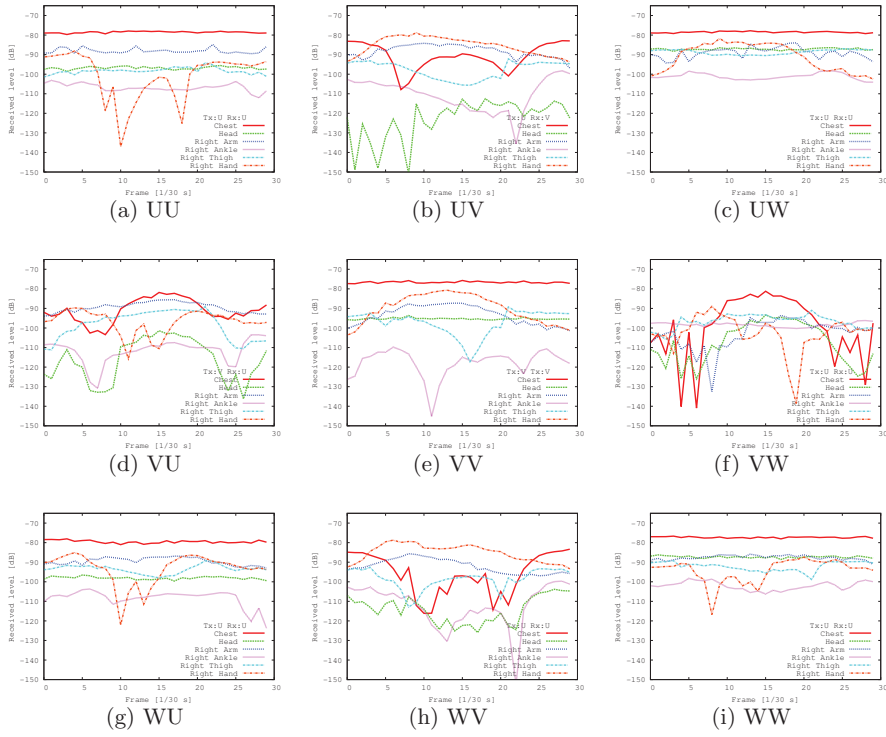


Figure 2: Temporal variations of received levels of the receivers during walking.

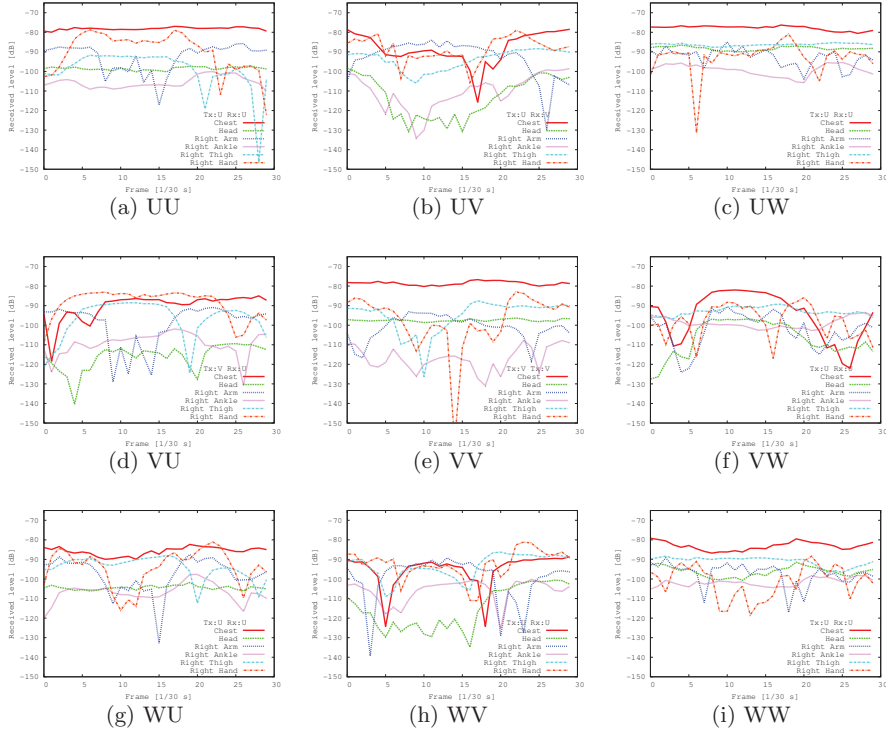
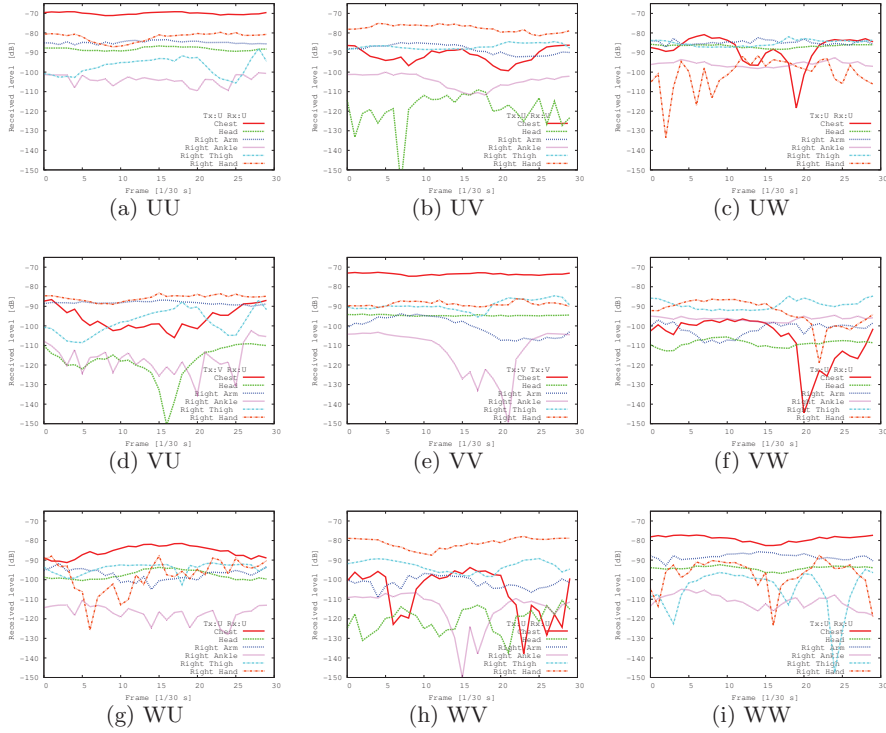


Figure 3: Temporal variations of received levels of the receivers during running.



**Figure 4: Temporal variations of received levels of the receivers during weak-walking.**

cases, and the dynamics shows minimum for the UW case. To design actual communication systems, dynamics are often problem because both too strong or too weak signal levels are inappropriate for receivers. As you can see in the Fig. 2, the walking scenario, the UW combination shows relatively stable and highest received level than the other cases. However, in the Fig. 3, the running scenario, the UW combination has a sharp signal drop at frame 6. We suppose that a diversity or other compensation technique is still necessary to continuous and reliable signal transmissions for dynamic BAN situations, even if antennas are optimized in directions or locations.

#### 4. STATISTICAL CHARACTERISTICS FOR 403.5 MHZ BAN PROPAGATIONS BY COMBINATIONS OF TX AND RX ANTENNA DIRECTIONS.

To design a BAN communication system, a propagation channel model is required. It is usually a stochastic model based on measurements. For example, the ref. [6] presents a statistical model for 4.5 GHz narrowband on-body propagation channel for specific human movements (walking and standing up/sitting down). As same as this paper, a transmitter was fixed on abdomen and receivers are fixed on several locations on body, and the best fit statistical distributions depended on the receiving locations and the movements. (tested distributions were Lognormal, Nakagami- $m$ , and Weibull distributions). In this paper, to consider the effects of antenna directions for transmitting and receiving

nodes, all movements and all receiver locations are modeled together. Fig. 5 shows the cumulative distributions of the received levels for all movements and all receiving locations by the combinations of TX-RX antenna direction. In the figure, both empirical and lognormal fitted cumulative distribution functions are shown in individual sub-figures. For all cases, lognormal distributions give very good fitting results. It is supposed that the fluctuation of the levels mainly caused by shadowings and mismatch of the antenna polarizations with temporal variation of human postures. Table 3 shows the fitted parameters ( $\mu$  and  $\sigma$ ) for the fitted curves in Fig. 5. As shown in the table, the largest  $\mu = -10.8$  is obtained for the UW polarization combination, and the smallest deviation  $\sigma = 1.246$  is obtained also for the UW case. The second best is the UU and the WW cases, which the polarizations coincide for the transmitting and the receiving antennas, however the difference to the other cases are not significant for these cases.

#### 5. CONCLUSIONS

In this paper, a consideration for polarization of both transmitting and receiving antennas in dynamic on-body networks at 403.5 MHz has been presented. The temporal level difference for the six human movements and the six receiving locations are calculated with the antenna directions  $\mathbf{u}$ ,  $\mathbf{v}$ , and  $\mathbf{w}$ . The statistical analysis shows that the overall level variations are well modeled by the lognormal fittings by individual combinations of the transmitting and the receiving antenna directions. It is shown that the UW combination of the antenna direction gives largest received level

TX-RX	UU	UV	UW	VU	VV	VW	WU	WV	WW
Mean	-97.5	-100.7	-93.8	-99.2	-98.0	-97.7	-98.6	-102.0	-97.5
Max	-83.2	-84.5	-81.6	-84.6	-83.8	-82.1	-84.2	-82.8	-82.2
Min	-149.7	-153.4	-133.5	-141.6	-142.2	-139.1	-154.0	-148.4	-156.7
Max-Min	66.5	69.0	51.8	57.0	58.4	57.0	69.9	65.6	74.5

Table 2: Mean, maximum, minimum, and dynamics of received levels for all TX–RX polarization combinations (all parameters are in dB).

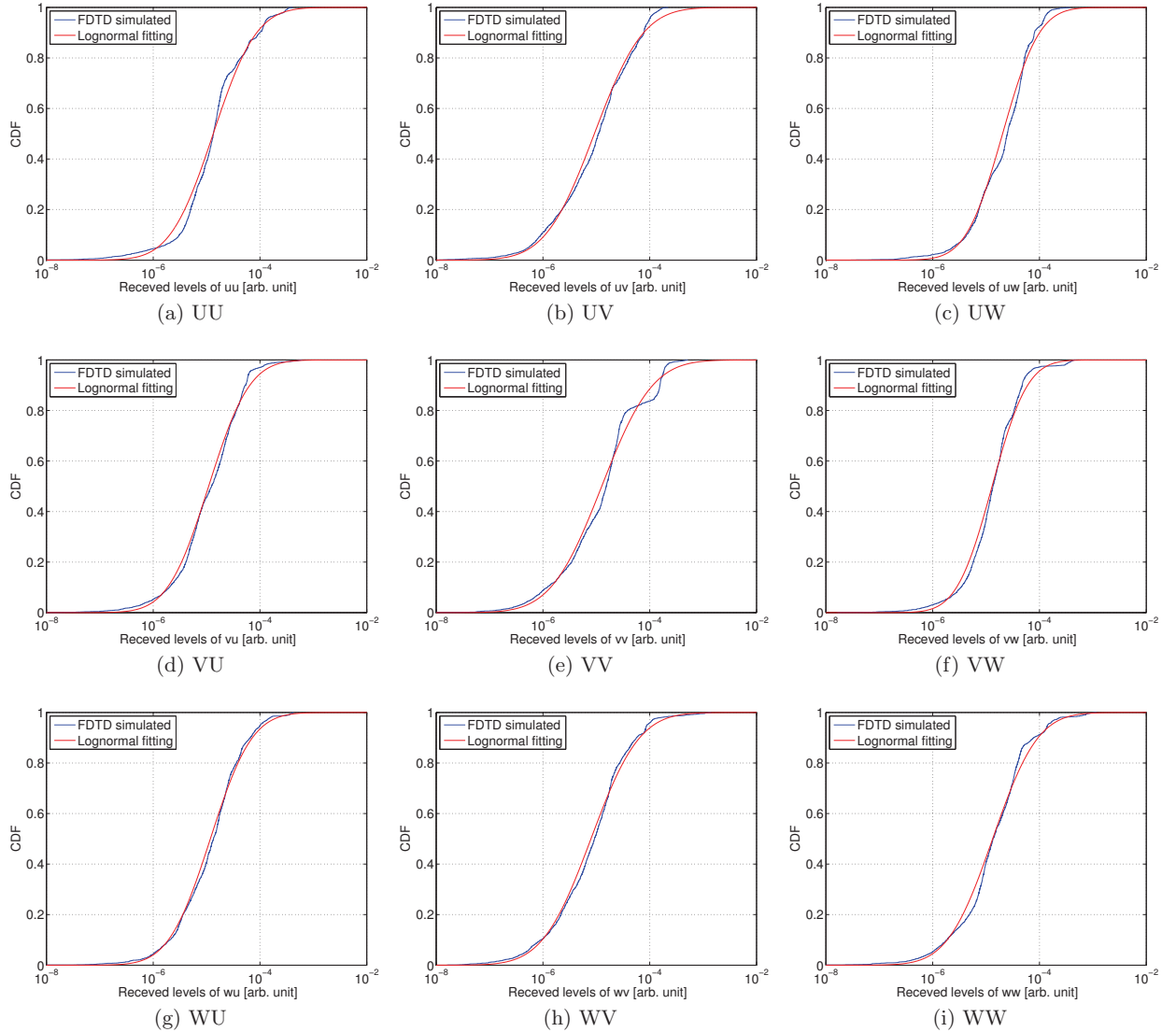


Figure 5: Cumulative Distribution Function for all movements and all receiving locations by the combinations of TX-RX antenna direction.

TX-RX	UU	UV	UW	VU	VV	VW	WU	WV	WW
$\mu$	-11.23	-11.6	-10.8	-11.42	-11.28	-11.25	-11.35	-11.74	-11.23
$\sigma$	1.465	1.66	1.246	1.388	1.72	1.197	1.415	1.641	1.53

**Table 3:** Parameters ( $\mu$ ,  $\sigma$ ) obtained by lognormal distribution fitting by TX-RX polarization combinations (all parameter are in arb. unit).

with smallest deviation, however, the differences between the other combinations are not significant. There are many things to do for the future works to utilize this results in actual BAN communication system designs. For examples, the followings are left for further study.

- Consideration for other frequencies (e.g. 950 MHz or 2450 MHz).
- Comparison with measurement results.
- Increase sampling time of movements to more rational statistical analysis
- Increase number of channels with consideration of multiple transmitter locations.
- Design and optimization of antennas for on-body networks for several frequencies.
- More realistic and useful dynamic on-body channel propagation modeling for BANs with considerations of antenna pattern or antenna de-embedding[9][2].

## 6. REFERENCES

- [1] A. Andrenko, I. Ida, and T. Kikuzuki. Dual-band patch antenna with monopole-like radiation patterns for ban communications. *Proc. 7th European Conf. on Antennas and Propagation (EUCAP 2013)*, pages 1922–1926, April 2013.
- [2] T. Aoyagi, M. Kim, and J. Takada. Characterization for a electrically small antenna in proximity to human body. *Proc. 7th European Conf. on Antennas and Propagation (EUCAP)*, pages 1–4, April 2013.
- [3] T. Aoyagi, M. Kim, J. Takada, K. Hamaguchi, and R. Kohno. Numerical simulations for wearable ban propagation channel during various human movements. *IEICE Trans. Commun.*, E94-B:2996–2500, September 2011.
- [4] M. Gallo, P. Hall, Q. Bai, Y. Nechayev, C. Constantinou, and M. Bozzetti. Simulation and measurement of dynamic on-body communication channels. *IEEE Trans. on Antennas and Propagation*, 59(2), February 2011.
- [5] M. Gallo, P. Hall, Y. Nechayev, and M. Bozzetti. Use of animation software in simulation of on-body communications channels at 2.45 ghz. *IEEE Antennas and Wireless Propagation Letters*, 7:321–324, July 2008.
- [6] M. Kim and J. Takada. Statistical model for 4.5-ghz narrowband on-body propagation channel with specific actions. *IEEE Antennas and Wireless Propagation Letters*, 8:1250–1254, 2009.
- [7] S. Swaisaenyakorn, P. Young, and J. Batchelor. Animated human movement and posture capture for body worn antenna simulation. *Proc. 5th European Conf. on Antennas and Propagation (EuCAP)*, pages 3791–3795, April 2011.
- [8] A. Taflove and S. Hagness. *Comutational Electrodynamics Third Edition*. Artech House, 2005.
- [9] J. Takada. De-emgedding of antennas from propagation channel in wireless communication. *Invited Lecture of 5th European Conf. on Antennas and Propagation (EuCAP)*, April 2011.
- [10] J. A. Zhang, D. B. Smith, L. W. Hanlen, D. Miniutti, D. R., and B. Gilbert. Stability of narrowband dynamic body area channel. *IEEE Antennas Wireless Propagat. Lett.*, 8:53–56, 2009.